Desalination and Water Treatment
www.deswater.com

1944-3994/1944-3986 © 2012 Desalination Publications. All rights reserved
doi: 10.1080/19443994.2012.677408

46 (2012) 115–123
August

Characterization of bio-char from pyrolysis of wheat straw and its evaluation on methylene blue adsorption

Yali Liu, Xiurong Zhao, Jianli Li, Dan Ma, Runping Han*

Department of Chemistry, Zhengzhou University, No. 100 Kexue Road, Zhengzhou 450001, P.R. China
Tel. +86 371 67781757; Fax: +86 371 67781556; email: rphan67@zzu.edu.cn

Received 26 July 2011; Accepted 20 February 2012

ABSTRACT

Bio-char, a by-product from the slow pyrolysis of wheat straw, was characterized and investigated as an adsorbent for the removal of cationic dye, methylene blue (MB) from solution. Elemental analysis, Fourier transform infrared spectrum, X-ray diffraction, and pH of point of zero charge (pH_{pzc}) were presented. Adsorption studies were performed at different pH, salt concentration, contact time and dye concentration in the batch mode. The results showed that there were—OH and other functional groups on the surface of bio-char and the pH_{pzc} of the bio-char was 7.8. The value of solution pH 8–9 was best for the MB adsorption quantity. Salt that coexisted in solution was not favored in MB adsorption. The equilibrium data were modeled with Langmuir, Freundlich, and Sips equations. Overall, the data were best fitted with the Sips model. The maximal adsorption capacity from the Sips model was 12.03 ± 0.41 mg/g at 293 K. Thermodynamic parameters were calculated and the results show that the process was spontaneous and endothermic in nature. Bio-char, a low-cost and eco-friendly adsorbent, can be used to adsorb the cationic dye from the solution.

Keywords: Adsorption; Bio-char; Methylene blue; Isotherm

1. Introduction

Dye wastewater discharged to natural receiving waters may make them unacceptable for public consumption due to the toxicological problems caused by the toxic dyes to the environment and to human health. Thus, it is desirable to eliminate dyes from textile wastewater [1]. Dye wastewater is usually treated by physical, chemical, and biological treatment processes. These include flocculation combined with flotation, membrane filtration, electrokinetic coagulation, electrochemical destruction, ion-exchange, irradiation, precipitation, ozonation, and biodegradation. However, these technologies are generally ineffective in color removal, expensive, and less adaptable to a wide range of dye wastewaters [1]. Adsorption is superior to other techniques in terms of initial cost, flexibility, and simplicity of design, ease of operation, and insensitivity to toxic pollutants. Furthermore, it can be used to remove different types of coloring materials. Its large-scale application is limited by the high cost of the adsorbent [2,3]. Use of activated carbon has been found to be effective, but it is too expensive and regeneration is difficult. Many studies have been undertaken to investigate the use of low-cost adsorbents. So, some raw or natural agricultural byproduct and carbonaceous materials based on this by-product as low-cost adsorbents have been tested to evaluate their efficiency in the removal of dyes and other pollutants [4–6]. However, some raw agricultural by-products have many disadvantages, one of these is the leaching of organic pollutants, which may cause

---

*Corresponding author.

further pollution [7]. This problem could be simply avoided by carbonization of the raw materials or chemical modification. Activated carbons, prepared from agricultural materials, had good adsorption capacities with respect to heavy metals, humic acid, phenol, and dyes [8]. The promising results were obtained when carbonaceous material prepared was utilized as adsorbent for wastewater treatment. The processing and transformation of agricultural residues into activated carbon or other products would alleviate problems of disposal and management of these waste by-products.

Bio-char is a pyrolytic by-product during bio-oil production. This oxygen-rich char is different from that formed by partial combustion. Alkali and alkaline earth cations remain in the condensed phase and are concentrated in the char [9]. In the field of biomass thermal conversion, attention has been focused on the liquid or gas product (bio-oil), but the bio-char, which is also an attractive byproduct, has received less attention. It is available for this carbonaceous residue used as soil amendment, except direct combustion for heat production [10]. The bio-char from pyrolytic process has been directly used as adsorbents for the removal of heavy metals [9,11]. But there are few papers about the removal of dyes from solution. Methylene blue (MB), one of the cationic dyes, has wider applications, which include coloring paper, temporary hair colorant, dyeing cottons, wools, and coating for the paper stock. The MB can cause eye burns, which may be responsible for permanent injury to the eyes of human beings and animals. Inhalation of MB can give rise to short periods of rapid or difficult breathing, while ingestion through the mouth produces a burning sensation and may cause nausea, vomiting, profuse sweating, and mental confusion [12]. So, the treatment of effluent containing this dye is of interest due to its harmful impact on receiving waters. In this paper, MB is selected as a model compound in order to evaluate the capacity of bio-char for the removal of dye from aqueous solutions.

As biomass pyrolysis to liquid and gas fuels is important in future, it can be estimated that large amounts of these chars will be available. Any use with a value in excess of its fuel value will be promising. Thus, this crude by-product char is easily obtained at low cost. The objective of this study was to study the feasibility of bio-char, obtained from slow pyrolytic processes of wheat straw, as adsorbents for cationic dye from solution. The aim was to find a value-added utilization approach for these by-products.

2. Materials and methods

2.1. Materials

Bio-chars were produced by slow pyrolysis of wheat straw in a fluidized reactor. Wheat straw was obtained from the local countryside. It was air-dried for 1 day and was ground and sieved to a particle size of 2 mm before use. The pyrolytic temperature is up to 550°C and the time through the fluidized bed is 5 min to produce bio-oil and bio-gas. The yield of bio-char is about 30% of wheat straw. Bio-chars as a by-product were ground and sieved and 20–40 mesh was selected as the adsorbent.

The formula of MB (C.I. No. 52015) is $C_{16}H_{18}ClN_3S\cdot 3H_2O$. The MB has a molecular weight of 373.9 g/mol. The stock solutions of MB were prepared in distilled water (500 mg/L). All working solutions were prepared by diluting the stock solution with distilled water to the desired concentration. The values of solution pH were near 7.7.

2.2. Characterizations of bio-char

The Fourier transform infrared (FTIR), pH_{pzc} (pH of zero point charge at the point of zero charge of the bio-char, namely the pH value required to give zero net surface charge), elemental analysis, specific surface area (from the N_2 adsorption isotherms), were presented.

The contents of carbon, hydrogen, and nitrogen were determined by elemental analysis instrument (Flash EA 1112, USA). Elemental compositions were obtained by X-ray fluorescence spectrometer (Philips PW 2404 X-ray fluorescence, Netherlands).

The functional groups present in the bio-char were characterized by a FTIR spectrometer (PE-1710, USA). Dried bio-char 10 mg was dispersed in 200 mg of spectroscopic grade KBr to record the spectra using potassium bromide disks to prepare the bio-char samples. The spectral range varied from 4,000 to 400 cm^{-1}.

X-ray diffraction (XRD) analysis was carried out to identify any crystallographic structure in the bio-char sample using a computer-controlled X-ray diffractometer.

The pH at point zero charge (pH_{pzc}) of bio-char, namely the pH value required to give zero net surface charge, was evaluated by the solid addition method. Initial pH values (pH_i) of 20 mL of 0.01 mol/L of KNO_3 solutions were roughly adjusted in the pH range of 2–10 on a PHS acidometer and were accurately noted. Then, 0.12 g of bio-char was added to each 50 mL conical flask and the flasks were placed in a thermostated water-bath shaker for overnight at 298 K. The final pH (pH_f) of the solutions separated by centrifugation was measured, and the pH_{pzc} was found at $\triangle pH = 0$ from a plot of $(pH_i - pH_f)$ vs. pH_i.

2.3. Adsorption procedure

Adsorption experiments were carried out in a rotary shaker at 100 rpm (293 K) using 50 mL shaking flasks containing 10 mL of different concentrations with 0.06 g of bio-char. The contact time is 7 h, except kinetic study. After adsorption, the samples were withdrawn from the flasks. The samples were then centrifuged and the leftout concentration in the supernatant solution was analyzed for measuring the MB absorbance using a UV/VIS-3000 spectrophotometer (Shimadzu Brand UV-3000) at a wavelength of maximum absorbance (668 nm).

The data obtained in batch model studies were used to calculate the MB uptake quantity. The quantity of MB adsorbed onto unit weight of adsorbent was calculated using the following equations, respectively:

$$q = \frac{V(c_0 - c)}{m} \tag{1}$$

where V is the solution volume (L), c_0 is the initial MB concentration (mg/L), c is the MB concentration at any time t (mg/L), and m is the mass of bio-char (g).

2.2.1. Effect of solution pH on adsorption

The effect of pH on values of q_e was analyzed over the pH range from 3 to 10. The initial pH values of the solutions were previously adjusted with 0.1 mol/L HNO_3 or NaOH solution. The initial concentration of MB was 100 mg/L.

2.2.2. Effect of contact time on adsorption

Batch adsorption tests were done at different contact time at the initial concentration of MB 100 mg/L with the initial pH 8–9. The flasks were then taken out at some intervals and the samples were centrifuged.

2.2.3. Effect of NaCl concentrations on adsorption

The effect of NaCl concentration (ionic strength) on adsorption was analyzed over the NaCl concentration range from 0 to 0.20 mol/L. The initial MB concentration was 100 mg/L and the solution pH was adjusted to 8–9.

2.2.4. The effect of MB concentration on adsorption

Adsorption isotherms studies were conducted in the MB concentration ranges of 10–150 mg/L. A series of such conical flasks was then shaken in a shaking water bath with temperatures 293, 303, and 313 K, respectively. Initial solution pH was adjusted to 8–9.

3. Results and discussions

3.1. Characterization of bio-char

3.1.1. Elemental analysis

The contents of elemental analysis for bio-char are C 63.11%, H 1.57%, 0.85% N, and 0 S, respectively. The solid residue of bio-char is 33.1% when bio-char is heated at 550℃ for one hour in an electric heating oven at air condition. So the bio-char was carbon rich and had carbon content. There are some inorganic elements confirmed by the X-ray fluorescence analysis, such as Si, K, Ca, Fe, Mg, Al, etc. The contents of these elements (as oxides) are SiO_2 13.08%, CaO 4.81%, K_2O 4.59%, MgO 2.55%, Fe_2O_3 2.11%, P_2O_5 1.25%, Cl 0.99%, and Al_2O_3 0.36%, respectively. The specific surface area of bio-char is 22.52 m^2/g.

3.1.2. FTIR analysis

FTIR analysis of the bio-chars was carried out to characterize the surface organic functional groups present on these samples. The FTIR spectrum of bio-char is shown in Fig. 1.

The bands in Fig. 1 are due to different surface groups. A broad absorption band around 3,423 cm^{-1} is attributed to the O–H stretching vibration of hydroxyl functional phenolic groups including hydrogen bonding due to adsorbed water. The absorption band near 2,900 cm^{-1} corresponds to the C–H stretching vibration from the methyl and methylene groups [11]. The peak at 1,564 cm^{-1} may be attributed to a C=C stretching vibration caused by the aromatic structure [13]. In the fingerprint region (1,500–910 cm^{-1}), the band near 1,425 cm^{-1} is attributed to O–H bending or C–O stretching vibration of phenol, while the bands at 1,384–1,402 cm^{-1} are assigned to C–H bending in alkanes/alkyl groups. The wavenumber near 1,063 cm^{-1} could be attributed to –C–O–C– stretching vibrations of polysaccharides or from the bending vibration of –C–OH. The peak near 874 cm^{-1} is characteristic of C–H bending vibration in a β-glucosidic linkage [14]. Another band was found at about 800 cm^{-1}, which is expected to be associated with the out-of-plane bending mode of O–H. The broad peak at 1,060, the peak at 800 cm^{-1}, and sharp peak at 461 cm^{-1} were also contributors to the adsorption from O–Si–O, indicating the presence of amounts of silica. This result is consistent with the content of 13.08% SiO_2 for bio-char.

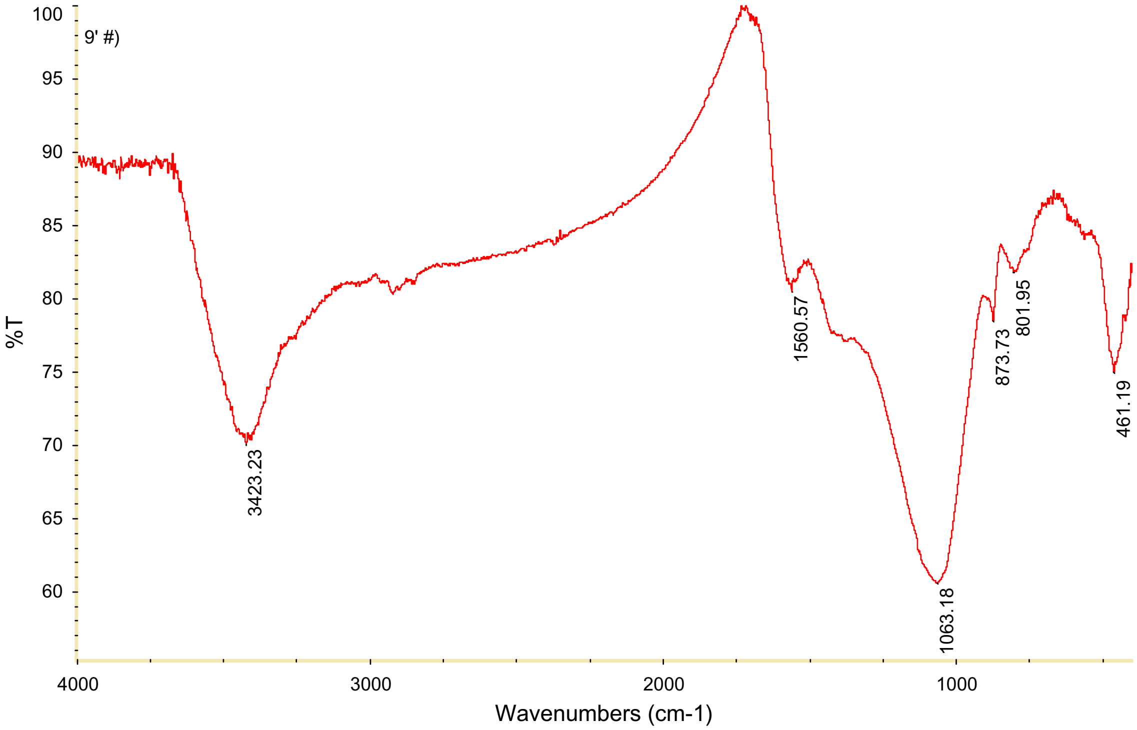

Fig. 1. FTIR of bio-char.

The observed spectra showed that bio-char produced consisted of several surface functional groups, which contributed positively to its color removal efficiency.

3.1.3. XRD analysis

Powder XRD patterns for the bio-char are recorded in Fig. 2. From Fig. 2, the peaks at $2\theta = 20^\circ$–30° refer to the stacking structure of aromatic layers (graphite 002), and the broadening has originated from the small dimensions of crystallites perpendicular to aromatic layers [15]. Sharp, non-labeled peaks in bio-char indicate miscellaneous inorganic components. Although not discussed in detail, the greater prevalence of these peaks is consistent with the higher content of SiO_2, CaO, and MgO. The sharp and the strongest peak at $2\theta = 26^\circ$ is originated from crystalline SiO_2. The X-ray diffraction peak confirmed that bio-char possesses a heterogeneous surface.

3.1.4. Zero point of charge

The pH of the zero point of charge (pH_{pzc}) of bio-char depends on the chemical and electronic properties of the functional groups on its surface. The results for determination of pH_{pzc} are shown in Fig. 3.

From Fig. 3, the pH_{pzc} value was approximately 7.8, and therefore pH values should be maintained above this value to ensure a negatively charged surface of bio-char and favor adsorption by electrostatic attraction between bio-char and the MB cationic ions. However, given the possibility of reaction with NaOH at high pH values, the maximum initial solution pH value performed in the present study was 10.

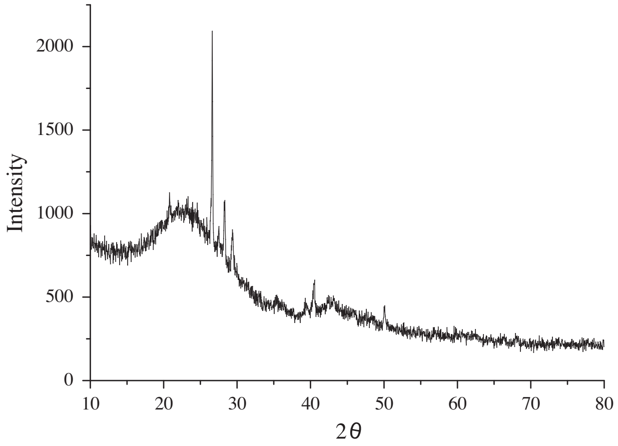

Fig. 2. XRD pattern of bio-char.

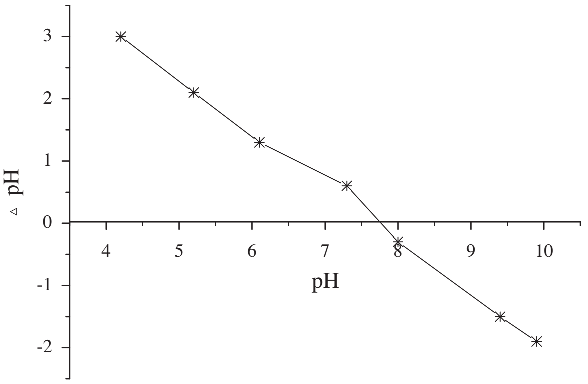

Fig. 3. Plots of △pH against initial pH for the determination of pH_{pzc} of bio-char.

3.2. Adsorption study

3.2.1. Effect of solution pH on adsorption quantity

The aqueous solution pH has been reported to present a significant influence on the adsorptive uptake of dyes due to its impact on both the surface binding sites of the adsorbent and the ionization process of the dye molecule. In the present study, the effect of pH was investigated between 3 and 10 and the results are displayed in Fig. 4.

From Fig. 4, it was observed that the solution pH affected adsorption quantity (q_e). The values of q_e increased with the pH value increasing in the range of 2.0–8.0. When the value of pH was from 8 to 9, the adsorption quantity changed little. So, the pH of the working solution was adjusted to 8–9. Apparently, the adsorption of MB prefers a higher solution pH value. Apparently, the higher the solution pH value (over the pH_{pzc} 7.8), the more the negative charges on the bio-char surface, the more attractive to cations on the bio-char surface. This is why a higher pH value is good for MB adsorption. From Fig. 4, adsorbent does not favor dye adsorption due to electrostatic repulsion when the pH value is smaller than 6, but even at pH = 3, the adsorption quantity was still over 50% compared to pH 8. This suggested that other actions, such as π–π dispersion interactions, be dominant in this case between bio-char and MB.

3.2.2. Effect of contact time on adsorption quantity

The results of adsorption quantity per gram rice husk (q_t) at different contact time (t) are shown in Fig. 5.

From Fig. 5, a three-stage kinetic behavior was evident: a rapid initial adsorption over 50 min, followed by a longer period of much slower uptake (300 min) and gradual equilibrium time. The first phase was the instantaneous adsorption stage or external surface adsorption. The second and third phase was the gradual adsorption stage and finally the MB uptake reached equilibrium.

3.2.3. Effect of NaCl concentration on adsorption quantity

The wastewater containing dye has a commonly higher salt concentration, and the effects of ionic strength are of some importance in the study of dye adsorption onto adsorbents. Fig. 6 shows the effect of NaCl concentration on the values of q_e.

From Fig. 6, it was seen that the increase in the salt concentration resulted in a decrease of values of q_e. This could be attributed to the competitive effect between MB positive ions and sodium cations from the salt for the sites available for the sorption process. Another reason is that as the ionic strength increases,

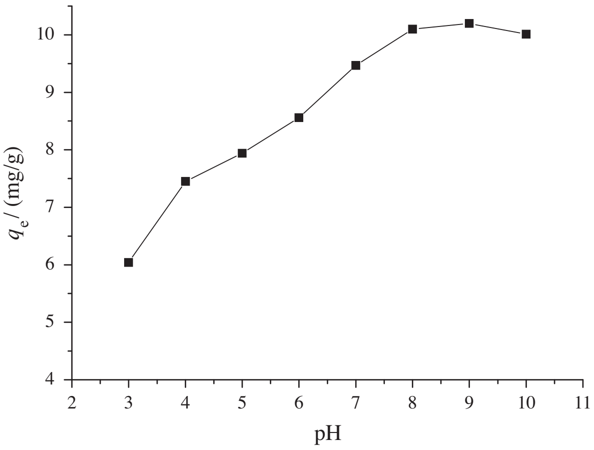

Fig. 4. The effect of pH on adsorption ($c_0 = 100$ mg/L).

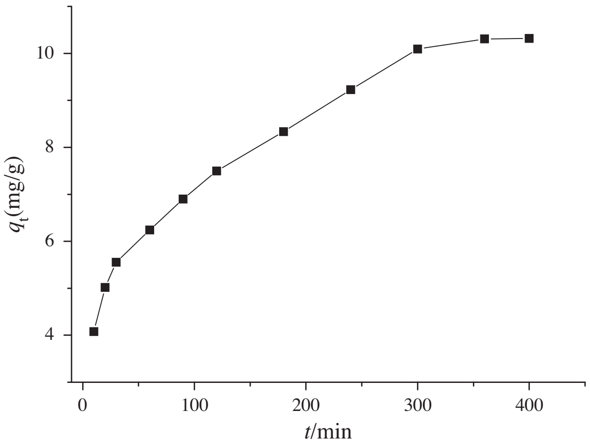

Fig. 5. The effect of contact time on adsorption ($c_0 = 100$ mg/L).

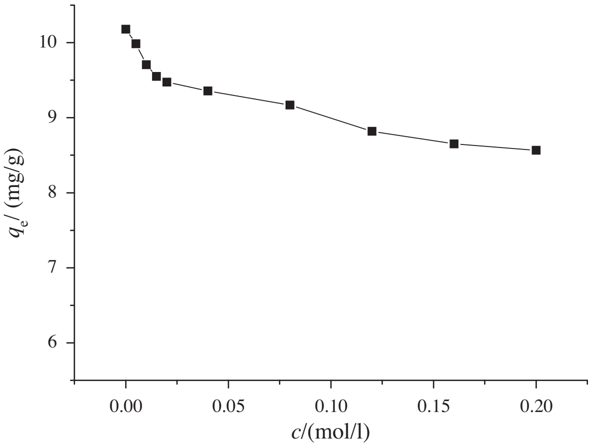

Fig. 6. The effect of NaCl concentration on MB adsorption ($c_0 = 100\,\text{mg/L}$).

the activity of MB and the active sites onto surface of bio-char decreases, so the adsorptive capacity of MB decreases. But even at 0.20 mol/L of salt, bio-char still has an adsorption capacity of 8.5 mg/g. So bio-char can be used to efficiently remove the MB from an aqueous solution with a higher salt concentration. Similar results were obtained by other studies [5,16].

3.2.4. The effect of equilibrium MB concentration on adsorption quantity

The effect of the equilibrium concentration of MB in the solutions on adsorption is shown in Fig. 7 (adsorption isotherm). As seen from Fig. 7, equilibrium uptake increased with the increase of MB concentrations at the range of experimental concentrations. This was a result of the increase in the driving force of the concentration gradient.

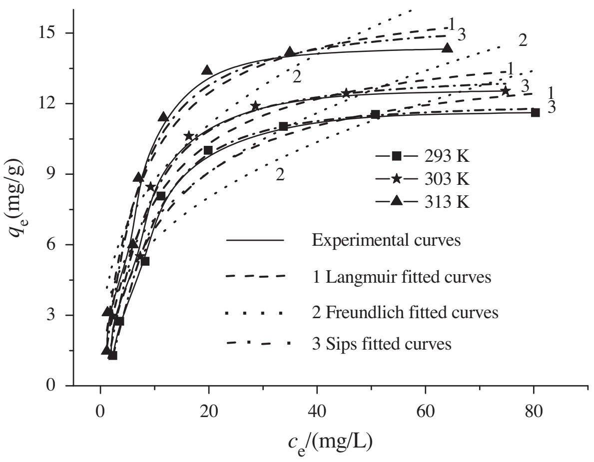

Fig. 7. Adsorption isotherms of MB adsorption onto bio-char.

The bigger adsorptive capacity of MB was also observed in the higher temperature range. This was due to the increasing tendency of adsorbate ions to adsorb from the solution to the interface with increasing temperature. The increase of the equilibrium adsorption quantity with increased temperature indicated that the adsorption of MB ions onto bio-char was endothermic in nature and adsorption is favored at a higher temperature.

3.3. Adsorption isotherm modeling and determination of thermodynamic parameters

3.3.1. Adsorption isotherm modeling

The design and efficient operation of adsorption processes require equilibrium adsorption data. The equilibrium isotherm model plays an important role in predictive results for the analysis and design of adsorption systems. Langmuir and Freundlich isotherm models are common and often applied. The relative parameters of each equation are obtained using least-square sum (SS) between the calculated data and experimental data by nonlinear regressive analysis. The calculated expression of SS is as follows.:

$$\mathrm{SS} = \sum (q_c - q)^2 \qquad (2)$$

where q_c is the predicted (calculated) quantity of MB adsorbed onto peanut husk according to adsorption models and q is the experimental data.

If higher value of R^2 and low value of SS are obtained, the model is good to predict the experimental data.

Langmuir equation [17]:

$$q_e = \frac{q_m K_L c_e}{1 + K_L c_e} \qquad (3)$$

where q_m is the q_e for a complete monolayer (mg/g), a constant related to adsorption capacity; and K_L is a constant related to the affinity of the binding sites and energy of adsorption (L/mg).

Freundlich equation [18]:

$$q_e = K_F c_e^{1/n} \qquad (4)$$

where K_F and $1/n$ are the Freundlich constants related to the adsorption capacity and adsorption intensity of the adsorbent, respectively.

Sips equation [19]:

$$q_e = \frac{q_{\max} (bC_e)^{1/m}}{1 + (bC_e)^{1/m}} \qquad (5)$$

where b and $1/m$ are model parameters.

The relative constants evaluated from the isotherms, the determined coefficients (R^2) and values of error (SS) are presented in Table 1. To assess the different isotherms and how they compare to experimental results, the theoretical plots for each isotherm are also presented with the experimental data for the adsorption of MB in Fig. 7.

From Table 1, the Sips model was best to fit the experimental data in the entire range of concentrations according to the values of R^2 and SS, combined with a comparison between fitted curves and experimental curves. It was observed from Fig. 7 that Sips isotherm was in good agreement with the experimental points at high-dye concentration. The weaknesses of the Langmuir isotherm were highlighted in the region of monolayer coverage, and the Freundlich isotherm was not able to characterize the adsorbent/adsorbate system in the entire range of concentrations. The values of q_m, K_L, K_F, and b increased with the temperature increasing, while the values of $1/n$ and 1/m decreased. The values of $1/n$ $(0.1 < 1/n < 1)$ indicated favorable adsorption of MB at experimental conditions.

Langmuir constant, q_m, represents the monolayer saturation at equilibrium. The values q_m about some adsorbent binding MB from the Langmuir constant are listed in Table 2. The capacity of adsorbent is relevant to surface property of adsorbent, adsorbate characterization, particle size, solution condition, and temperature. Compared to other adsorbents for MB removal and activated carbon [20–27], the values of q_m were not larger. Furthermore, the adsorption capacity of bio-char for MB adsorption is smaller than that of the natural wheat straw [22]. But bio-char, a by-product from bio-oil production process, is of low-cost, easily obtained, and causes no leaching of organic pollutants. Furthermore, it presented good adsorption capacity in comparison to other low-cost residues. So, it is still feasible to employ bio-char as an adsorbent for the MB removal from aqueous solutions.

Table 1
Parameters of adsorption isotherm models for MB adsorption

Isotherm constants	Temperature (K)		
	293	303	313
Langmuir			
K_L (L/mg)	0.089 ± 0.020	0.110 ± 0.025	0.140 ± 0.031
q_m (mg/g)	14.16 ± 0.12	14.98 ± 1.06	16.92 ± 1.17
R^2	0.958	0.957	0.962
SS[a]	0.814	0.967	1.134
Freundlich			
K_F	2.64 ± 0.79	3.14 ± 0.87	3.96 ± 0.97
$1/n$	0.371 ± 0.082	0.355 ± 0.078	0.344 ± 0.073
R^2	0.836	0.837	0.847
SS	3.22	3.75	4.59
Sips model			
q_m (mg/g)	12.03 ± 0.41	13.26 ± 0.83	15.65 ± 1.34
b	0.123 ± 0.010	0.140 ± 0.021	0.162 ± 0.033
$1/m$	1.68 ± 0.19	1.46 ± 0.27	1.27 ± 0.28
R^2	0.991	0.976	0.969
SS	0.209	0.652	1.11

As bio-char can undergo direct combustion, the loaded-dye bio-char is not regenerated and can be mixed with coal to be combustion for heat production. This content will undergo studied in further research.

3.3.2. Thermodynamic parameters of adsorption

The free energy change (ΔG^0), enthalpy change (ΔH^0), and entropy change (ΔS^0) were determined according to equilibrium data. The apparent equilibrium constant (K'_c) of the adsorption is defined as [28]:

$$K'_c = \frac{c_{ad,e}}{c_e} \tag{6}$$

where $c_{ad,e}$ is the concentration of MB on the adsorbent at equilibrium (mg/L). The value of K'_c can be obtained with the lowest experimental MB concentration. The K'_c value is used in the following equation to determine the Gibbs free energy change of adsorption (ΔG^0).

$$\Delta G^0 = -RT \ln K'_c \tag{7}$$

The enthalpy (ΔH^0) and entropy (ΔS^0) can be obtained from the slope and intercept of a van't Hoff equation of ΔG^0 vs. T:

$$\Delta G^0 = \Delta H^0 - T\Delta S^0 \tag{8}$$

where ΔG^0 is the standard Gibbs free energy change, J; R is the universal gas constant, 8.314 J/mol K and T is the absolute temperature, (K).

The thermodynamic parameters are listed in Table 3.

The negative values of ΔG^0 at various temperatures are due to the fact that the adsorption processes are spontaneous. The increase in the absolute value of ΔG^0 as the temperature rises indicates that the affinity of MB on bio-char is higher at high temperature. The lower values of ΔG showed that the adsorption pro-

Table 2
MB adsorption by various materials: q_m obtained from the Langmuir constant

q_m(mg/g)	Adsorbent	References
5.87	Coir pith carbon	[20]
66.0	Coconut-husk-based activated carbon	[20]
472	Straw activated carbon	[20]
980	Commercial activated carbon	[21]
0.84	Corncob-based activated carbon	[22]
19.94	Natural Zeolite	[23]
20.3	Cereal chaff	[5]
11.8	Indian Rosewood sawdust	[24]
80.9	Phoenix tree leaves	[25]
16.56	Wheat shell	[26]
60.66	Wheat straw	[27]
12.03	Bio-char	This study

Table 3
Thermodynamic parameters of MB adsorption

Thermodynamic parameters	Temperature (K)		
	293	303	313
ΔG^0 (kJ/mol)	−2.97	−3.59	−5.30
ΔH^0 (kJ/mol)		31.2	
ΔS^0 (kJ/mol K)		0.115	

cess may be a physical process. The enhancement of adsorption capacity of the adsorbent at higher temperatures may be attributed to an enlargement of pore size and/or activation of the adsorbent surface. The positive value of ΔH^0 indicates the endothermic nature of the process, whereas the positive ΔS^0 value confirms the increased randomness at the solid–solute interface during adsorption and reflects the affinity of the adsorbent material for dye. The low value of ΔH^0 shows that the effect of temperature is not significant at the range of studied temperatures, while the low value of ΔS^0 also indicates that no remarkable change on entropy occurred during the adsorption process.

4. Conclusions

There were several surface functional groups on the surface of bio-char and the value of pH_{pzc} is 7.8. It was the advantage of MB adsorption at higher pH value, while common salt that coexisted in solution was not favored in MB adsorption. The experimental data were best fitted with the Sips model and the maximal adsorption capacity was 12.03 ± 0.41 mg/g at 293 K from the Sips model. The process was spontaneous and endothermic.

Acknowledgments

I thank the referees' and editor's suggestion and correction to improve the quality of this paper. This work was supported by the National Natural Science Foundation of China for undergraduate cultivation in basic science (J0830412), the Natural Science Foundation of Henan Province (92300410232).

Appendix

The structure of MB is following:

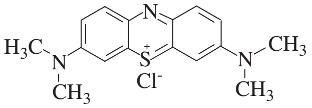

References

[1] T. Robinson, G. McMullan, R. Marchant, P. Nigam, Remediation of dyes in textile effluent: A critical review on current treatment technologies with a proposed alternative, Bioresour. Technol. 77 (2001) 247–255.

[2] V.K. Gupta, Suhas, Application of low cost adsorbents for dye removal—a review, J. Environ. Manage. 90 (2009) 2313–2342.

[3] G. Crini, Non-conventional low-cost adsorbents for dye removal: A review, Bioresour. Technol. 97 (2006) 1061–1085.

[4] M.M. Abd El-Latif, Amal M. Ibrahim, Removal of reactive dye from aqueous solutions by adsorption onto activated carbons prepared from oak sawdust, Desalin. Water Treat. 20 (2010) 102–113.

[5] R.P. Han, Y.F. Wang, P. Han, J. Shi, J. Yang, Y.S. Lu, Removal of methylene blue from aqueous solution by chaff in batch mode, J. Hazard. Mater. 137 (2006) 550–557.

[6] W.H. Zou, P. Han, Y.L. Lia, X. Liu, X.T. He, R.P. Han, Equilibrium, kinetic and mechanism study for the adsorption of neutral red onto rice husk, Desalin. Water Treat. 12 (2009) 210–218.

[7] W.S. Wan Ngah, M.A.K.M. Hanafiah, Removal of heavy metal ions from wastewater by chemically modified plant wastes as adsorbents: A review, Bioresour. Technol. 99 (2008) 3935–3948.

[8] O. Ioannidou, A. Zabaniotou, Agricultural residues as precursors for activated carbon production—a review, Renew. Sust. Energy Rev. 11 (2007) 1966–2005.

[9] D. Mohan, C.U. Pittman, Jr, M. Bricka, F. Smith, J. Mohammad, P.H. Steele, M.F. Alexandre-Franco, V. Gómez-Serrano, H. Gong, Sorption of arsenic, cadmium, and lead by chars produced from fast pyrolysis of wood and bark during bio-oil production, J. Colloid Interface Sci. 310 (2007) 57–73.

[10] J.W. Lee, M. Kidder, B.R. Evans, S. Paik, A.C. Buchanan Iii, C.T. Garten, R.C. Brown, Characterization of biochars produced from corn stovers for soil amendment, Environ. Sci. Technol. 44 (2010) 7970–7974.

[11] D. Mohan, S. Rajput, V.K. Singh, P.H. Steele, C.U. Pittman, Jr. Modeling and evaluation of chromium remediation from water using low cost bio-char, a green adsorbent, J. Hazard. Mater. 188 (2011) 319–333.

[12] I.A.W. Tan, A.L. Ahmad, B.H. Hameed, Adsorption of basic dye using activated carbon prepared from oil palm shell: Batch and fixed bed studies, Desalination 225 (2008) 13–28.

[13] D. Ozcimen, F. Karaosmanoglu, Production and characterization of bio-oil and biochar from rapeseed cake, Renew. Energy 29 (2004) 779–787.

[14] K.A. Krishnan, A. Haridas, Removal of phosphate from aqueous solutions and sewage using natural and surface modified coir pith, J. Hazard. Mater. 152 (2008) 527–535.

[15] H. Takagi, K. Maruyama, N. Yoshizawa, Y. Yamadab, Y. Sato, XRD analysis of carbon stacking structure in coal during heat treatment, Fuel 83 (2004) 2427–2433.

[16] J.Y. Song, W.H. Zou, Y.Y. Bian, F.Y. Su, R.P. Han, Adsorption characteristics of methylene blue by peanut husk in batch and column mode, Desalination 265 (2011) 119–125.

[17] I. Langmuir, The constitution and fundamental properties of solids and liquids, J. Am. Chem. Soc. 38 (1916) 2221–2295.

[18] H.M.F. Freundlich, Uber die adsorption in losungen, Z. Phys. Chem. 57 (1906) 385–470.

[19] R. Sipss, On the structure of a catalyst surface, J. Chem. Phys. 16 (1948) 490–495.

[20] M. Rafatullah, O. Sulaiman, R. Hashim, A. Ahmad, Adsorption of methylene blue on low-cost adsorbents: A review, J. Hazard. Mater. 177 (2010) 70–80.

[21] N. Kannan, M.M. Sundaram, Kinetics and mechanism of removal of methylene blue by adsorption on various carbons—a comparative study, Dyes Pigments 51 (2001) 25–40.

[22] R.L. Tseng, S.K. Tseng, F.C. Wu, Preparation of high surface area carbons from corncob using KOH combined with CO_2 gasification for the adsorption of dyes and phenols from water, Colloids Surf. A 279 (2006) 69–78.

[23] R.P. Han, J.J. Zhang, P. Han, Y. Wang, Z.H. Zhao, M.S. Tang, Study of equilibrium, kinetic and thermodynamic parameters about methylene blue adsorption onto natural zeolite, Chem. Eng. J. 145 (2009) 496–504.

[24] V.K. Garg, M. Amita, R. Kumar, R. Gupta, Basic dye (methylene blue) removal from simulated wastewater by adsorption using Indian Rosewood sawdust: A timber industry waste, Dyes Pigments 63 (2004) 243–250.

[25] R.P. Han, W.H. Zou, W.H. Yu, S.J. Cheng, Y.F. Wang, J. Shi, Biosorption of methylene blue from aqueous solution by fallen phoenix tree's leaves, J. Hazard. Mater. 141 (2007) 156–162.

[26] Y. Bulut, H. Aydın, A kinetics and thermodynamics study of methylene blue adsorption on wheat shells, Desalination 194 (2006) 259–267.

[27] Y.J. Wu, L.J. Zhang, C.L. Gao, J.Y. Ma, X.H. Ma, R.P. Han, Adsorption of copper ions and methylene blue in single and binary system on wheat straw, J. Chem. Eng. Data 54 (2009) 3229–3234.

[28] Z. Aksu, Determination of the equilibrium, kinetic and thermodynamic parameters of the batch biosorption of nickel(II) ions onto *Chlorella vulgaris*, Process Biochem. 38 (2002) 89–99.